Enhanced efficiency ultraviolet $LiY_xLu_{1-x}F_4:RE^{3+}$ (RE = Ce,Yb) laser

2014 Laser Phys. Lett. 11 125807

(http://iopscience.iop.org/1612-202X/11/12/125807)

IOP Publishing | Astro Ltd Laser Physics Letters

Laser Phys. Lett. **11** (2014) 125807 (5pp) doi:10.1088/1612-2011/11/12/125807

Enhanced efficiency ultraviolet $LiY_xLu_{1-x}F_4:RE^{3+}$ (RE = Ce,Yb) laser

L A Nurtdinova and S L Korableva

Kazan Federal University, Kremlevskaya st. 18, Kazan 420008, Russia

E-mail: ne.goruj@gmail.com

Received 7 October 2014
Accepted for publication 8 October 2014
Published 30 October 2014

Abstract

We report the results of laser tests in $LiY_xLu_{1-x}F_4:RE^{3+}$ (RE = Ce, Yb; x = 0, 0.3) crystals and the effect on laser characteristics (slope efficiency and tuning range) of such variations of the lasing conditions as the pumping repetition rate, temperature and additional illumination of the active element. It was established that slope efficiency increases and the tuning range of ultraviolet lasing widens and becomes continuous when the crystal is cooled down below 0 °C, or exposed to 532 nm radiation. 266 and 340 nm illumination reduces or completely quenches laser oscillation. The photodynamic processes underlying these effects, such as excited-state absorption and formation/destruction of color centers, are discussed.

Keywords: UV laser, fluoride crystals, mixed crystals, rare earth ions, excited-state absorption, color centers, photodynamic processes

(Some figures may appear in colour only in the online journal)

1. Introduction

$LiYF_4$ (YLF) and $LiLuF_4$ (LLF) single crystals as well as their solid solutions, doped with various rare-earth (RE) ions, are not only well-known and studied materials for quantum electronic devices, but remain highly demanded and prospective active media for the lasers to date (see, for example, [1–4]). Doped with Ce^{3+} ions these crystals represent a not very large group of solid-state materials capable of lasing directly in the ultraviolet (UV) spectral region. However, all RE-activated dielectric crystals (and especially UV-emitting ones) experience various photodynamic processes (excited-state absorption (ESA), color centers (CC) formation and so on) when exposed to UV light.

Certain attempts to eliminate the harmful influences of photodynamic processes have been made before. Thus, a coactivation of RE-doped active media with various RE ions, providing a recombination channel for the freed by UV light charge carriers, that would otherwise be trapped by the numerous defects of the lattice, has been proved successful [5]. Furthermore, enhanced efficiency and continuous tunability of lasing wavelength by the cooling of an active element below the room temperature have been already achieved in Ce:LLF crystal before [6]. The advantages of mixed crystals lie in the enhanced distribution coefficient of the impurity ions [7], lesser CC formation and, consequently, higher gain [8], wider tuning range and lower cost.

Here we report the results of laser tests in $LiY_{0.3}Lu_{0.7}F_4:Ce^{3+}$/$Ce^{3+}$ + Yb^{3+} in comparison with $LiLuF_4:Ce^{3+}$ monocrystals and the effect on laser characteristics (slope efficiency and tuning range) of such variations of the lasing conditions as the pumping repetition rate, temperature and additional illumination of the active element.

2. Experimental details

$LiY_{0.3}Lu_{0.7}F_4:Ce^{3+}$ + Yb^{3+} (Ce,Yb:LYLF), $LiY_{0.3}Lu_{0.7}F_4:Ce^{3+}$ (Ce:LYLF) and $LiLuF_4:Ce^{3+}$ (Ce:LLF) crystals were grown using the Bridgeman–Stockbarger technique in graphite crucibles at the Kazan Federal University. The samples used in our measurements were identical 8 × 1.5 mm polished disks of crystals containing a nominal 1% concentration of substitutional Ce^{3+} and Yb^{3+} ions and were oriented such that the c axis was lying in the disk plane.

Laser tests were carried out in a flat Fabry–Perot resonator (3.5 cm for nonselective and 5.5 cm for selective configuration) using a quasi-longitudinal geometry. Ce^{3+} ions were excited by π-polarized 300 nm laser pulses, provided by one of the Stokes components of the H_2-Raman cell, pumped in turn by the 4th harmonic of the Nd:YAG laser (10 Hz, ~10 nsec pulse width). 300 nm is near the maximum of the lowest 4f–5d absorption band of Ce^{3+} ions and its optical density is ~2.3 along the 15 mm path length of the sample. A 20 cm focal-length quartz lens was used to focus the pumping beam to a 1 mm diameter spot. Optimization of the output coupler was performed using mirrors with 16%, 25%, 65% and 80% reflectivity. Tuning of the laser wavelength was achieved using fused silica 60° prism.

Additional π-polarized 532 nm, 266 nm and σ-polarized 340 nm laser beams (of 0.95, 0.5 and 0.5 energy density), provided by the same Nd:YAG laser and Raman cell, were focused into 2.5 × 2.5, 1.1 × 1.1 and 1.5 × 1.5 mm spots, so they have interacted with the pumped volume of the sample. All these wavelengths are off resonance with 4f–5d transitions of trivalent cerium ions.

Cooling of laser elements down to −20 °C was carried out by blowing vapors of liquid nitrogen onto the sample installed in contact with the calibrated thermistor on the copper holder. The whole resonator was covered by the styrofoam cap. The range of temperature variation was limited by the frosting of the sample's surfaces. Unless stated otherwise, the experiments were performed at room temperature. Pumping repetition rate was varied using a mechanical external shutter from 0.1 to 10 Hz.

3. Results and discussion

Free running laser operation in nonselective resonator was observed at 310 nm for all three samples and laser emission was found to be almost completely π-polarized. The highest output power in nonselective resonator was obtained using an R = 25% output coupler. In this case the slope efficiency was ~20% and the threshold to laser oscillation was ~0.4 mJ. Figure 1 shows the output power performance from the Ce:LYLF laser.

In a selective resonator, tuning of the lasing wavelength was achieved (see figures 2(*a*) and (*b*)) for all three samples with an R = 80% output coupler. However, none of the samples provided a continuous tuning curve and between the short- and longer-wavelength maxima no lasing was observed. Short-wavelength lasing (~ 305–316 nm) was completely π-polarized, intense and stable, whereas long-wavelength radiation (~ 323–331 nm) was partially σ-polarized and its intensity fluctuated depending on the portion of σ-polarized radiation in it. Such polarization peculiarities are, probably, connected with the much larger absorption of π-polarized rather than σ-polarized radiation by CC in this spectral region [9] and, hence, the higher gain for the σ-polarized light [6, 8].

The highest energy and slope efficiency of lasing was demonstrated by Ce:LLF, however Ce,Yb:LYLF provided the most stable long-wavelength lasing with the less pronounced polarization features. Tuning ranges in these two samples are approximately the same, although slightly shifted towards shorter wavelengths for the Ce,Yb:LYLF sample. In Ce:LYLF, tunability was obtained only for the short-wavelenght wing of the tuning curve.

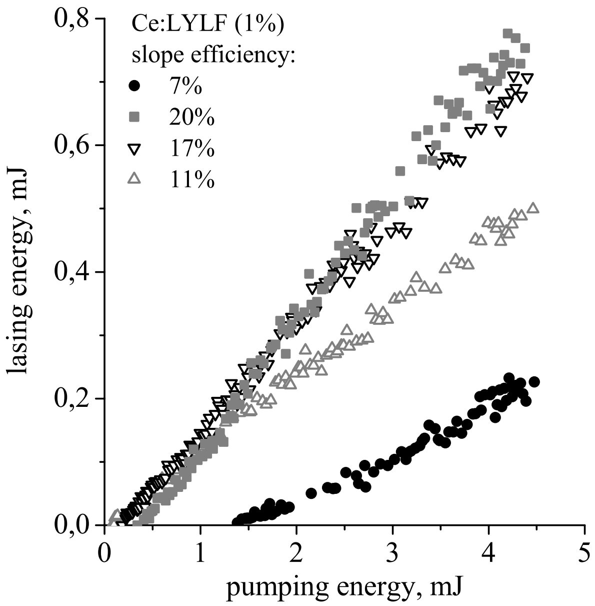

Figure 1. 310 nm lasing slope efficiency in Ce:LYLF crystal in a nonselective resonator for the various reflectivities (R) of the output coupler: R = 16% (•), R = 25% (■), R = 65% (∇), R = 80% (△).

Lowering of temperature of the active element from 27 down to −20 °C, however, resulted in a considerable improvement of laser characteristics in all three materials. In figure 3(*a*), the dependence of maximal lasing energy at a given pumping energy from the temperature of the active element is presented. It is obvious that lasing energy monotonically increases by 30–50% while temperature decreases down to −20 °C. Slope efficiency also increases with the lowering of temperature from 20 to 30–35% depending on the sample (see figure 3(*b*)). Moreover, the tuning range in Ce,Yb:LYLF crystal widened, while in Ce:LYLF tuning in the long-wavelength wing was obtained.

It would seem that the apparent positive influence of cooling the laser element on its lasing characteristics is mainly due to the processes of absorption from the excited states of Ce^{3+} ions. According to the earlier developed model of photodynamic processes in the studied materials [10] excited-state absorption transitions of the active ions do not occur directly to the conduction band, but to the higher-lying states of the impurity ion itself (6s, most likely). These transitions are followed by the relaxation of the excited carriers to the conduction band and their capture by the various crystalline defects with the formation of CC. Indeed, pumping wavelength (300 nm) falls at the edge of the excited-state photoionization band centered at 270 nm [10]. Thus, lowering of temperature results in the narrowing of the vibration-broadened spectrum of the 6s levels of Ce^{3+}. This in turn leads to the lowering of the ESA transition probability and, therefore, lasing efficiency increases.

Seeking to further improve that model additional illumination of the active elements by 266 nm laser pulses simultaneous to pumping ones has been performed. 266 nm radiation should coincide well with the excited-state photoionization band near its maximum, therefore, illumination of the pumped

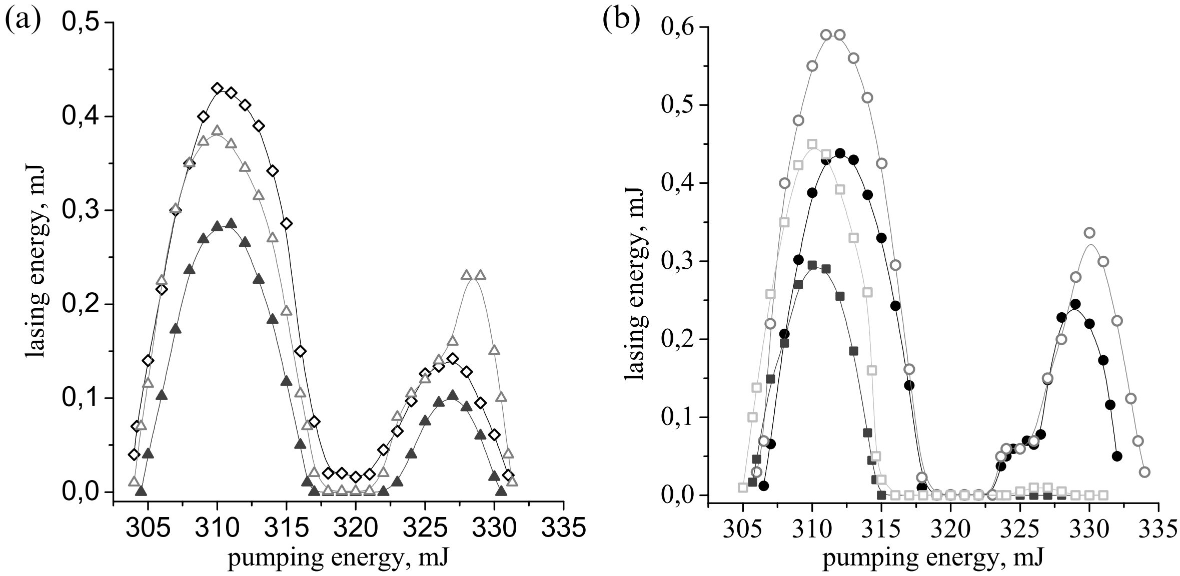

Figure 2. Tuning of laser wavelength in a selective resonator with an R = 80% output coupler obtained in (*a*) Ce,Yb:LYLF crystal: T = 300 K (▲), T = 263 K (△), with illumination at 532 nm (◇); (*b*) Ce:LLF: T = 300 K (•), T = 273 K (○); Ce:LYLF: T = 300 K (■), T = 273 K (□).

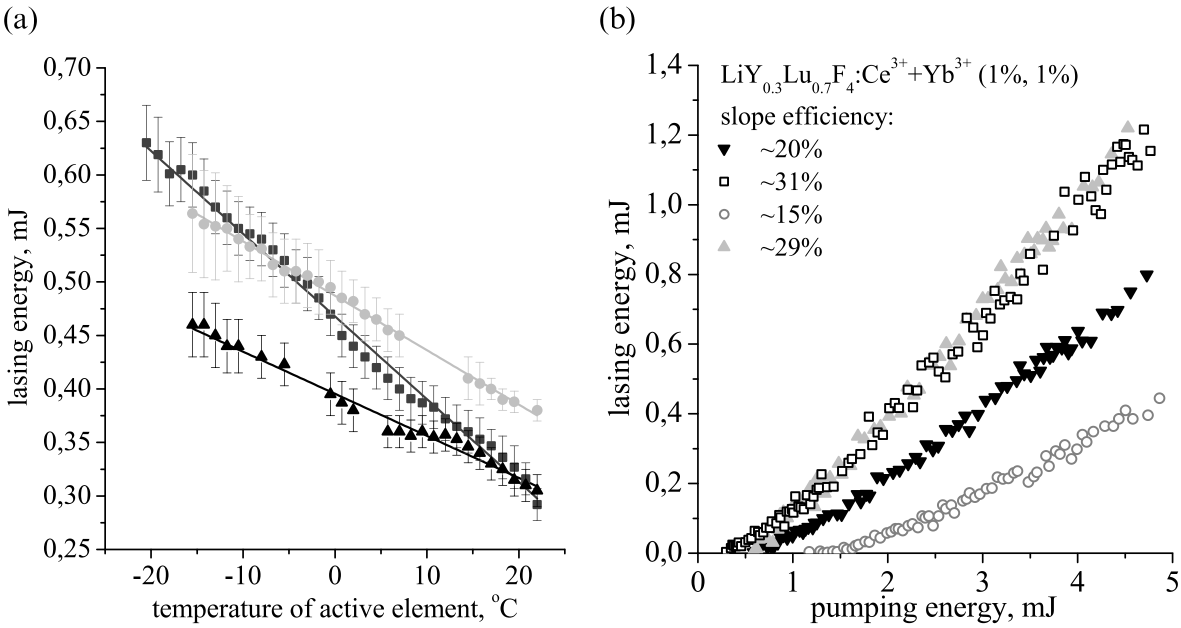

Figure 3. (*a*) Variation of 310 nm lasing energy with the decrease of temperature: Ce:LLF (•), Ce:LYLF (■), Ce,Yb:LYLF (▲). (*b*) Slope efficiency of 310 nm lasing in nonselective resonator in Ce,Yb:LYLF crystal: T = 300 K (▼), T = 267 K (▲), 532 nm illumination (□), 266 nm illumination (○).

portion of the sample with the appropriate energy density should result in a depletion of the upper laser level.

As can be seen from figure 4(*b*), illumination of the sample by the σ-polarized 266 nm radiation leads to the considerable (at least 50%) lowering of lasing energy and slope efficiency. The least susceptibility to 266 nm radiation was demonstrated by the Ce:LLF sample, whereas in Ce:LYLF crystal lasing was completely suppressed. In order to rule out the possible influence of CC absorption at 266 nm, the dependence of 266 nm radiation absorption by the pumped volume of the sample from the 300 nm pumping energy was registered. The fitting procedure using function, established by finding the steady-state analytical solution for the four-level rate-equation system (including two Ce levels, conduction band level and a level of CC), was performed. The best fit was achieved when 266 nm absorption only included excited-state transitions from the Ce^{3+} upper state to the conduction band and the worst when only bleaching of CC by 266 nm light with no regard to ESA was considered. Therefore, despite the bleaching effect that, according to [9], 266 nm light should have on stable F-centers, the depletion of upper laser level population by strong ESA seems to be more efficient. It should be noted

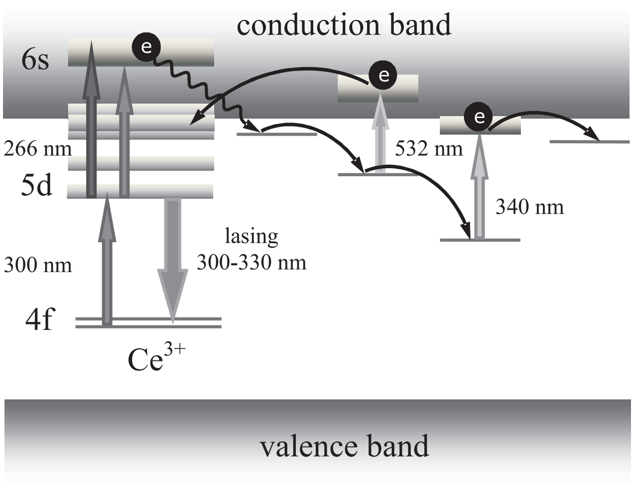

Figure 4. Model of photodynamic processes in $LiY_XLu_{1-X}F_4:RE^{3+}$ (RE = Ce,Yb) crystals.

that suppression of lasing by 266 nm illumination is much more pronounced when the probing radiation is σ- rather than π-polarized, which correlates well with the polarization peculiarities of the cooling effect [6].

In order to shift the equilibrium towards the enhanced bleaching of UV-induced CC the additional illumination of the active elements by pulsed radiation at 340 and 532 nm was performed. According to the published researches 340 nm and 532 nm radiation coincide well with the absorption bands of the F- [11] and either M- [12] or R- [13] type CC, respectively. It was expected that bleaching of CC by the applied radiation would result in the release of trapped carriers back into the lasing channel. However, the illumination at 340 nm resulted in the further deterioration of laser output in the investigated crystals (although less pronounced than the effect of 266 nm radiation with the similar energy density). Since 340 nm light does not coincide with Ce^{3+} absorption bands and the photoconductivity edge falls at 300 nm in these crystals [10], there are only two possibilities of how 340 nm light may affect Ce^{3+} lasing: the upper laser level's population depletion and CC absorption. However, no reduction of cerium's luminescence was observed after the 340 nm radiation was turned on. Besides, since radiative transition probability near 340 nm is considerably lower than that near the maxima of the gain contour, the deteriorating effect would have been rather less pronounced.

On the other hand, F-centers in YLF have a wide absorption band between 300–400 nm (peaking at 340 nm) [9], much more intense for π rather than σ polarization, so they should absorb lasing radiation in a long-wavelength wing better than in a short-wavelength one of the tuning curve. Illuminating the sample in a selective cavity we observed that short-wavelength lasing efficiency was reduced while the long-wavelength one was completely suppressed for the same levels of lasing and illuminating energy densities. Therefore, it is reasonable to suggest that the effect of 340 nm radiation is stipulated by the CC. We propose the following model for this effect (see figure 4). Indeed, stable CC described in [9] are formed by very deep traps with the lifetime of several days. They efficiently absorb 355 nm light, though cannot be bleached by it, but can be bleached by 325 nm radiation. So following the absorption of 340 nm radiation by these centers, captured electrons find themselves in the excited state not more than 3000 cm^{-1} below the conduction band. From there they can be nonradiatively transfered to the shallow traps with the activation energy of 4200 and 4500 cm^{-1} [9] and with rather shorter lifetimes (ns, μs, ms). These transient CC, apparently, absorb generated lasing radiation more efficiently. Either way, captured electrons are not being released to participate in the lasing.

Table 1. Slope efficiencies of 310 nm lasing for the different lasing conditions.

	Ce:LLF (%)	Ce:LYLF (%)	Ce,Yb:LYLF (%)
$T = 300$ K, no illumination	20	21	20
266 nm illumination	15.5	—	12.5
532 nm illumination	35	32	29
$T = 267$ K, no illumination	28	32	30

Illumination of the active element by 532 nm radiation, nevertheless, turned out to be more advantageous. Slope efficiency of 310 nm lasing increased by 50% with the decreasing of lasing threshold and widening of tuning range (see figures 3(*a*) and (*b*)). Since investigated materials are completely transparent towards 532 nm radiation when no UV pumping is applied and there is no ESA possible at that wavelength, bleaching of shallow transient CC by 532 nm radiation is apparently responsible for the considerable improvement of laser characteristics in this case.

Slope efficiency of 310 nm lasing in all three investigated materials under various experimental conditions are presented in figure 3(*b*) and table 1.

Decrease of the repetition rate of pumping pulses from 10 down to 0.1 Hz has also resulted in the slight increase of slope efficiency of 310 nm lasing by 3–5%, probably since the increased period between pulses leaves a better chance for longer-living CC to decay. At the same time it was noticed that after a while (several tens of minutes) lasing energy decreases by approximately 10% of the value it took after the active element was subjected to the light bleaching stable CC and does not decline further afterwards. Therefore, reduction of the repetition rate did not benefit lasing considerably, but indicates nonetheless that stable CC though reduce the overall efficiency of Ce,Yb:LYLF crystal based lasers, but do not further affect it in the long run. The majority of loss is caused, thereby, by the transient absorptions (either from the excited-states of Ce ions themselves, or by the short-lived CC).

4. Conclusion

Tunable UV lasing in $LiY_XLu_{1-X}F_4:RE^{3+}$ (RE = Ce,Yb; $x = 0$, 0.3) crystals have been achieved. Maximal slope efficiency in nonselective resonator at 310 nm was 21% in normal conditions, increased to 35% and 32% with the use of additional

532 nm illumination and lowering of the active element's temperature, considerably decreased (down to 12% and even to complete suppression of lasing) with the use of additional 340 and 266 nm irradiation. Tunability of UV lasing was improved by the lowering of temperature and with the use of 532 nm illumination, mainly, due to it getting continuous over the whole tuning range. Besides, lasing in longer-wavelength range was achieved for the Ce:LYLF crystal that was absent in normal conditions as opposed to the Ce,Yb:LYLF one, demonstrating the practical benefits of Yb-codoping. On the whole, Ce:LLF crystal demonstrated higher output in both selective and non-selective configurations, but Ce,Yb:LYLF crystal revealed more stable lasing in the longer wavelength wing of the tuning curve, where polarization peculiarities have been observed.

Analysis of the possible mechanisms underlying the observed phenomena allowed the suggestion that dramatic change in UV lasing characteristics under 266 nm illumination is essentially associated with the ESA, depleting the upper laser levels population, whereas effects caused by 340 and 532 nm irradiation are due to the various types of color centers, induced in these materials by UV pumping. Decrease of pumping repetition rate from 10 to 0.1 Hz did not lead to any considerable changes in laser performance. Stable color centers only contribute to the initial drop of lasing energy, while major losses are determined by the dynamic processes, associated with ESA and transient color centers.

Therefore, we have demonstrated that varying certain lasing conditions (temperature or illumination of the active element) it is possible to shift the dynamic equillibrium between lasing and photodynamic processes, contributing to the loss. This can be used not only to improve laser output of the active media, but to create such quantum electronic devices as saturable absorber or Q-switch with the dynamically variable characteristics.

Acknowledgments

Authors are grateful to M Marisov for the preparation of samples, V Semashko for the idea of the research, A Naumov for the permission to use the Raman-shifter and A Nizamutdinov for the helpful discussions. The research was supported by RFBR, research project No 12-02-31578 and the subsidy allocated to Kazan Federal University for the state assignment in the sphere of scientific activities in 2013-2014.

References

[1] Bolanos W, Starecki F, Braud A, Doualan J-L, Moncorge R and Camy P 2013 *Opt. Lett.* **38** 5377
[2] Li H, Liu X, Wu J, Zhang X and Li Y 2012 *Laser Phys.* **22** 523–6
[3] Li C, Zhang X, Liang W and Zhao Z 2011 *Laser Phys.* **21** 340–2
[4] Hansen N-O, Bellancourt A-R, Weichmann U and Huber G 2010 *Appl. Opt.* **49** 3864–8
[5] Bensalah A, Nikl M, Vedda A, Shimamura K, Satonaga T, Sato H, Fukuda T and Boulon G 2002 *Radiat. Eff. Defects Solids* **157** 56367
[6] Johnson K S and Coutts D W 2003 *Proc. SPIE* **5137** 28–36
[7] Nizamutdinov A, Semashko V, Naumov A, Korableva S and Marisov M 2010 *JETP Lett.* **91** 21–3
[8] Nizamutdinov A, Nurtdinova L, Semashko V and Korableva S 2014 *Opt. Spectrosc.* **116** 732–8
[9] Lim K S and Hamilton D S 1989 *J. Opt. Soc. Am.* B **6** 1401–6
[10] Nurtdinova L, Semashko V, Guyot Y, Korableva S, Joubert M-F and Nizamutdinov A 2011 *Opt. Mater.* **33** 1530–4
[11] Renfro G M, Halliburton L E, Sibley W A and Belt R F 1980 *J. Phys. C: Solid State Phys.* **13** 1941–50
[12] Nikanovich M V, Shkadarevich A P, Tipenko Yu S and Umreiko D S 1993 *J. Appl. Spectrosc.* **58** 143–8
[13] Peakheart D W 1998 *Radiat. Eff. Defects Solids* **143** 213–24